Tunable Isolated Attosecond X-ray Pulses with Gigawatt Peak Power from a Free-Electron Laser

Joseph Duris,[1,*] Siqi Li,[1,2,*] Taran Driver,[1,3,4] Elio G. Champenois,[3] James P. MacArthur,[1,2] Alberto A. Lutman,[1] Zhen Zhang,[1] Philipp Rosenberger,[1,3,5,6] Jeff W. Aldrich,[1] Ryan Coffee,[1] Giacomo Coslovich,[1] Franz-Josef Decker,[1] James M. Glownia,[1] Gregor Hartmann,[7] Wolfram Helml,[6,8,9] Andrei Kamalov,[2,3] Jonas Knurr,[3] Jacek Krzywinski,[1] Ming-Fu Lin,[1] Jon P. Marangos,[4] Megan Nantel,[1,2] Adi Natan,[3] Jordan O'Neal,[3,2] Niranjan Shivaram,[1] Peter Walter,[1] Anna Wang,[3,10] James J. Welch,[1] Thomas J. A. Wolf,[3] Joseph Z. Xu,[11] Matthias F. Kling,[1,3,5,6] Philip H. Bucksbaum,[1,3,2,10] Alexander Zholents,[11] Zhirong Huang,[1,10] James P. Cryan,[1,3,†] and Agostino Marinelli[1,‡]

[1]*SLAC National Accelerator Laboratory, Menlo Park, CA, 94025, USA*

[2]*Physics Department, Stanford University, Stanford, CA, 94305, USA*

[3]*Stanford PULSE Institute, SLAC National Accelerator Laboratory, Menlo Park, CA, 94025, USA*

[4]*The Blackett Laboratory, Imperial College, London, SW7 2AZ, UK*

[5]*Max Planck Institute of Quantum Optics, D-85748 Garching, Germany*

[6]*Physics Department, Ludwig-Maximilians-Universität Munich, 85748 Garching, Germany*

[7]*Institut für Physik und CINSaT, Universität Kassel, Heinrich-Plett-Str. 40, 34132 Kassel, Germany*

[8]*Zentrum für Synchrotronstrahlung, Technische Universität Dortmund, Maria-Goeppert-Mayer-Straße 2, 44227 Dortmund, Germany*

[9]*Physik-Department E11, Technische Universität München, James Franck-Straße 1, 85748 Garching, Germany*

[10]*Applied Physics Department, Stanford University, Stanford, CA, 94305, USA*

[11]*Argonne National Laboratory, Lemont, IL, 60439, USA*

Abstract

The quantum mechanical motion of electrons in molecules and solids occurs on the sub-femtosecond timescale. Consequently, the study of ultrafast electronic phenomena requires the generation of laser pulses shorter than 1 fs and of sufficient intensity to interact with their target with high probability. Probing these dynamics with atomic-site specificity requires the extension of sub-femtosecond pulses to the soft X-ray spectral region. Here we report the generation of isolated soft X-ray attosecond pulses with an X-ray free-electron laser. Our source has a pulse energy that is a million times larger than any other source of isolated attosecond pulses in the soft X-ray spectral region, with a peak power exceeding 100 GW. This unique combination of high intensity, high photon energy and short pulse duration enables the investigation of electron dynamics with X-ray non-linear spectroscopy and single-particle imaging, unlocking a path towards a new era of attosecond science.

* These authors contributed equally to this work.

† To whom correspondence should be addressed: jcryan@slac.stanford.edu

‡ To whom correspondence should be addressed: marinelli@slac.stanford.edu

INTRODUCTION

The natural time scale of electron motion in molecular systems is determined by the binding energy, I_p, typically between 8 and 12 eV. Quantum mechanics tells us that this relationship is given by $\tau = \hbar/I_p$, where $\hbar$ is the reduced Planck constant. Therefore, the relevant time scale for electron motion in molecular systems is on the order of a few hundred attoseconds (1 as $= 10^{-18}$ sec). Light pulses approaching this extreme timescale were first demonstrated in 2001 [1]. These early demonstrations employed a process called high harmonic generation (HHG), where a strong, infrared laser-field was used to coherently drive electrons in an atomic or molecular gas, leading to high-order harmonic up-conversion of the driving laser field [2–5]. The extension of time-resolved spectroscopy into the attosecond domain has greatly advanced our understanding of electron dynamics in atoms, molecules, and condensed matter systems [6–8]. This attosecond revolution has been almost exclusively driven by HHG based sources [1, 9–20], which have been recently extended to reach the soft X-ray wavelengths (above 280 eV [21]) and produce the shortest pulses ever recorded [22–25]. Extending attosecond pulse sources into the soft X-ray domain is particularly important because soft X-rays can access core-level electrons whose absorption properties are sensitive probes of transient electronic structure [26–28].

In parallel with the development of HHG, the last two decades have seen the rise of X-ray free-electron lasers (XFELs), such as the Linac Coherent Light Source (LCLS), as the brightest sources of X-ray radiation [29–35]. The working principle of an XFEL is based on the interaction of a relativistic electron beam with an X-ray electric field in a long periodic array of magnetic dipoles called an undulator [36–38]. The radiation/electron interaction causes the electron beam to reorganize itself in a sequence of microbunches shorter than the radiation wavelength, which results in the coherent emission of X-ray radiation with a peak power many orders of magnitude larger than the spontaneous level [37, 38]. Compared to laser-based HHG sources, XFELs have a large extraction efficiency at X-ray wavelengths—typically of order 0.1% or larger. With a typical electron beam peak power in the tens of terawatts range, the resulting X-ray pulses have tens of gigawatts of peak power, several orders of magnitude larger than table-top X-ray sources. Furthermore, the photon energy of FEL sources is easily tunable via small configuration changes of the accelerator or the undulator. The shortest pulse achievable with an XFEL is limited by the available amplifica-

tion bandwidth, which is of similar magnitude to their extraction efficiency $\leq 0.1\%$ [36, 39]. For example, the X-ray bandwidth of LCLS can support pulses shorter than 1 fs for hard X-ray energies [40, 41]. However, the shortest possible pulse duration increases to 1-2 fs for photon energies below 1 keV [42, 43], where the relevant core-level absorption edges for light elements are found: carbon (280 eV), nitrogen (410 eV), and oxygen (540 eV). In this letter, we report the generation and time-resolved measurement of gigawatt-scale isolated attosecond soft X-ray pulses with an XFEL. The bandwidth limitation of the XFEL was overcome by compressing the electron beam with a high-power infrared pulse, a technique termed enhanced self-amplified spontaneous emission (ESASE) [44].

Figure 1 shows a schematic representation of our experimental setup named X-ray laser-enhanced attosecond pulse generation (XLEAP). The energy distribution of the electron beam is modulated by the resonant interaction with a high-power infrared pulse in a long-period undulator (or wiggler) [44–46]. This modulation is converted into one or more high-current ($\sim$ 10 kA) spikes by a magnetic chicane. The spikes are subsequently used in the undulator to generate short X-ray pulses. This bunch compression method effectively broadens the XFEL bandwidth and allows the generation of sub-fs pulses in the soft X-ray spectral region. In our experiment, rather than using an external infrared laser as originally proposed by Zholents [44], we employ the coherent infrared radiation emitted by the tail of the electron beam in the wiggler to modulate the core of the electron beam [47, 48]. This method results in a phase-stable, quasi-single-cycle modulation, and naturally produces a single high-current spike that can generate an isolated attosecond pulse. Figures 1 (a-d) show the measured initial current profile and the evolution of the phase-space of the core of the electron bunch during the three stages of ESASE compression.

After separating the broad bandwidth X-ray pulses from the spent electron bunch, the X-ray pulses are focused and temporally overlapped with a circularly polarized, 1.3 μm, infrared (IR) laser field in a velocity map imaging (VMI) spectrometer [49]. Photoelectrons ionized by the X-ray pulse receive a "kick" proportional to the vector potential of the IR laser pulse at the time of ionization [50]. Through the interaction of the ionized electron with the dressing IR-laser field, the temporal properties of the X-ray pulse are mapped onto the final momentum distribution of the emitted photoelectrons [51–53]. This technique was originally called the "attosecond streak camera," and is routinely used to measure the temporal profile of isolated attosecond pulses from HHG sources [54]. In contrast to

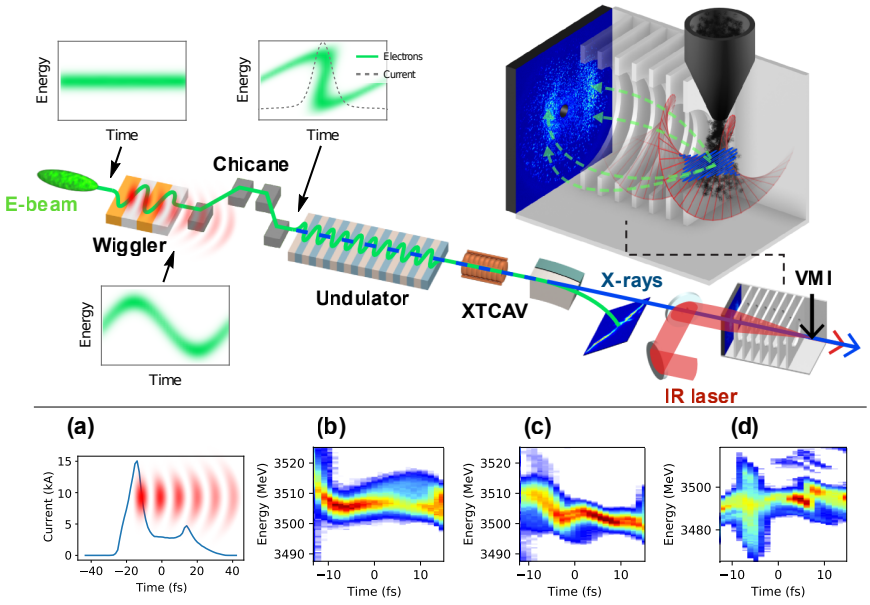

FIG. 1. **Top: schematic representation of the experiment.** The electron beam travels through a long period (32 cm) wiggler and develops a single-cycle energy modulation. The energy modulation is turned into a density spike by a magnetic chicane and sent to the LCLS undulator to generate sub-fs X-ray pulses. After the undulator the relativistic electrons are separated from the X-rays and sent to a transverse cavity (labeled XTCAV) used for longitudinal measurements of the beam. The X-rays are overlapped with a circularly polarized infrared laser (labeled IR laser) and interact with a gas-jet to generate photoelectrons. The extracted photoelectrons are streaked by the laser and detected with a velocity map imaging (VMI) spectrometer. The momentum distribution of the electrons is used to reconstruct the pulse profile in the time domain. **Bottom: measurements of the ESASE modulation process.** (a) the measured current profile of the electron bunch generated by the accelerator. The tail of the bunch has a high-current horn that generates a high-power infrared pulse used for the ESASE compression. (b), (c) and (d) Show the longitudinal phase-space of the core of the electron bunch in three different conditions: (b) with no wiggler and no chicane we measure the electron distribution generated by the accelerator; (c) after inserting the wiggler we observe a single-cycle energy modulation generated by the interaction between electrons and radiation; (d) after turning on the chicane the modulation is turned into a high current spike at t = -5 fs.

measurements done with HHG sources, in this work we are able to diagnose the single-shot pulse profile, rather than an average pulse shape. Moreover, the shot-to-shot fluctuations (or jitter) in the relative arrival time between the X-ray and optical field present at an FEL facility [55] makes single-shot measurements unavoidable. This single shot measurement scheme was originally demonstrated at LCLS by Hartmann *et al.*, who recovered the "time-energy structure" of SASE pulses produced by LCLS [43]. We have adapted this technique to measure the sub-femtosecond structure of the X-ray pulses produced by XLEAP.

RESULTS

Figure 2 (a) shows a single-shot measurement of the "streaked" photoelectron momentum distribution, which we use to reconstruct the full temporal profile of the X-ray pulse [53]. The raw data is filtered and down-sampled (Fig. 2 (b)) before being fed into the reconstruction algorithm, which returns a pulse profile and corresponding photoelectron distribution (Fig. 2 (c)). The robustness of this algorithm has been tested at length in Ref. [53], and is detailed in the supplemental material. Figure 2 also shows representative temporal profiles retrieved from the reconstruction at photon energies of 905 eV (panel d) and 570 eV (panel e). Figures 2 (f) and (g) show the distribution of pulse widths (full width at half maximum of the intensity profile) retrieved from two large data sets at these photon energies. The data shows that the XLEAP setup generates sub-femtosecond X-ray pulses, and we find a median duration of 284 as FWHM (476 as) at 905 eV (570 eV). The pulse duration fluctuates on a shot-to-shot basis and half of the single-shot measurements fall within a 106 as (166 as) window at 905 eV (570 eV). This amount of fluctuations is consistent with numerical simulations of ESASE FEL operation (see e.g. [56]). The estimated uncertainty on the single-shot pulse duration is between 10% and 30% of the measured duration depending on the pulse energy and the amplitude of the streaking laser field (a discussion on the experimental uncertainty of the measurement can be found in the supplemental materials). The median pulse energy is 10 μJ at 905 eV and 25 μJ at 570 eV. However, due to the intrinsic fluctuations of SASE FELs [39] we observe pulses well above the mean value (up to 250 μJ for 570 eV, corresponding to a peak power in the hundreds of GW). We note that for the 570 eV dataset we were only able to obtain converging reconstructions for pulse energies higher than 130 μJ, corresponding to the top 8%. However, since the data at both energies

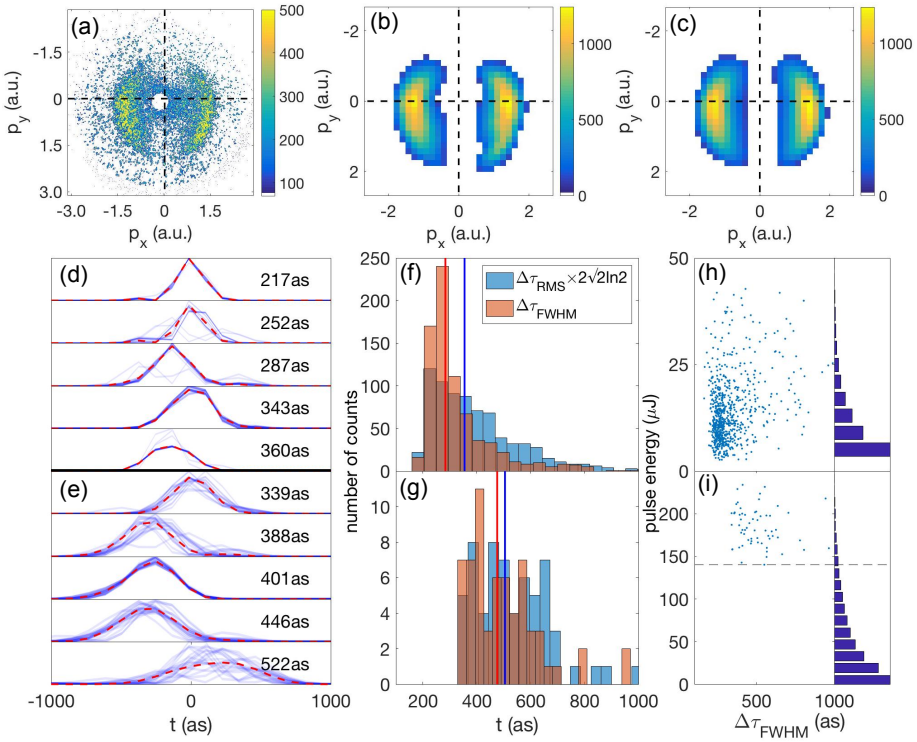

FIG. 2. **Results of the angular streaking measurement.** (a,b,c): measured and reconstructed streaked photoelectron distribution from a single X-ray pulse. Our reconstruction algorithm reads the photoelectron momentum distribution (a), downsamples the data (b) and fits it to simulated streaked spectra calculated from a complete basis set (c). (d,e) Representative pulse reconstruction at 905 eV (d) and 570 eV (e). The shaded blue lines represent the solutions found from running the reconstruction algorithm initiated by different random seeds, and the red lines represent the most probable solution (see Supplementary Material for details). The labeled number is the averaged $\Delta\tau_{\mathrm{FWHM}}$ over the different solutions. (f,g): distribution of retrieved X-ray pulse durations for 905 eV (f) and 570 eV (g). The red and blue vertical lines correspond to the median of $\Delta\tau_{\mathrm{FWHM}}$ and $\Delta\tau_{\mathrm{RMS}} \times 2\sqrt{2\ln 2}$ respectively. For 905 eV data, they are 284 as and 355 as. For 570 eV data, they are 476 as and 505 as. (h,i): scatter plot of pulse energy as a function of pulse duration for the reconstructed shots and a histogram of the pulse energy for the entire data set for 905 eV (h) and 570 eV (i).

does not show a significant correlation between pulse energy and duration (Figure 2 panels (b) and (e)) we believe that the average pulse duration from this sample is representative of the entire data set.

In a separate set of experiments we measured single-shot X-ray spectra with a grating spectrometer. Figure 3 shows a range of single-shot X-ray spectra recorded around 650 eV and 905 eV, and the distribution of the measured bandwidth (FWHM). The median FWHM bandwidth is 7.5 eV and 5 eV for the 905 eV and 650 eV datasets respectively. The Fourier transform limited (FTL) duration for a bandwidth of 7.5 eV (5 eV) is 240 as (365 as). The average pulse duration recovered from our reconstruction at similar energies is within a factor of 2 of the FTL value. This discrepancy is due to the beam-energy chirp introduced by longitudinal space-charge forces within the high-current ESASE spike [57]. This results in a residual chirp in the emitted X-rays, which is reproduced in the reconstruction (see Supplemental Materials). Ripples in the spectral intensity are visible in the 650 eV spectra and are due to interference with satellite pulses. The pulse energies of these side pulses can be inferred from the single-shot spectra and are typically less than 0.3% of the main pulse for 650 eV and negligible for 905 eV.

CONSIDERATIONS FOR PUMP/PROBE SPECTROSCOPY

To put the results of our work in context, we detail the development of isolated attosecond pulse sources in Figure 4, where we compare the measured pulse energy from existing attosecond light sources with the requisite flux to saturate the ionization of $1s$ electrons in various atomic systems. The saturation level serves as a coarse approximation to the energy required for a pump/probe experiment, and sources within two orders of magnitude of saturation are likely useful for pump/probe studies. The pulse energy produced by HHG sources decays very rapidly with the photon energy and is several orders of magnitude below the threshold for non-linear interaction in the soft X-ray range ($E > 280$ eV). Conversely our method can produce isolated attosecond pulses with tens of μJ of pulse energy, increasing the available pulse energy at soft X-ray wavelengths by six orders of magnitude, and reaching intensities sufficient for attosecond pump/attosecond probe experiments. Note that Fig. 4 reports the pulse energy measured for the experiments shown in Figs. 2 and 3, as well as other experiments using the XLEAP setup at different photon energies. The highest observed median pulse energy is ~ 50 μJ.

In addition to high single pulse photon flux, the application of this technique to attosecond pump/attosecond probe experiments requires the generation of pairs of synchronized pulses.

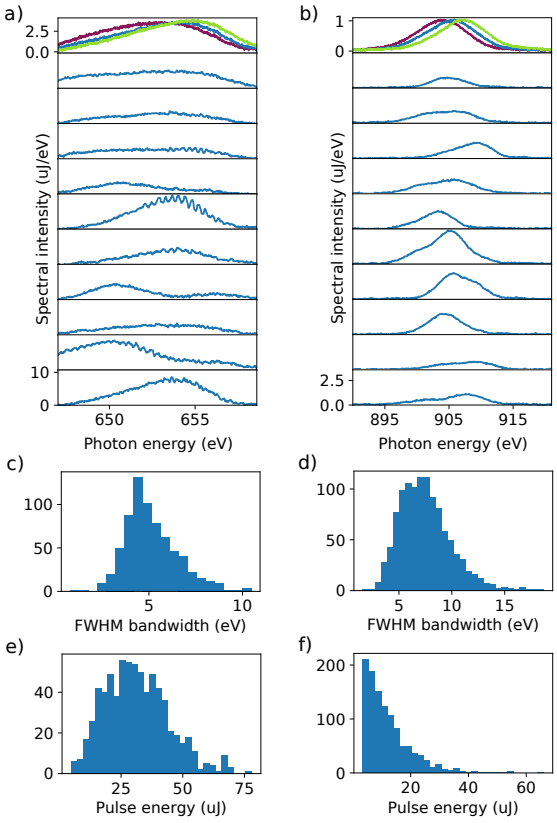

FIG. 3. **Spectral measurements** (a,b) Spectra of the attosecond X-ray pulses measured with a grating spectrometer at two different electron beam energies ((a): 3782.1 MeV; (b): 4500.3 MeV). The top figures show average spectra at slightly different electron beam energies (in steps of 2.7 MeV for 650 eV and 3.0 MeV steps for 905 eV), while the remaining spectra show single-shot measurements at the energy of the center curves shown in the top plots. (c,d): histogram of the distribution of FWHM bandwidths. Panels (e,f) show a histogram of the distribution of pulse energies.

Ideally these pulses could have different photon energies allowing for excitation at one atomic site in a molecular system to be probed at another [58]. To this end, ESASE can be easily adapted to generate pairs of pulses of different colors using the split undulator method [59–61]. In this scheme the LCLS undulator is divided in two parts separated by a magnetic chicane, as shown at the top of Fig. 5. The ESASE current spike is used to generate two X-ray pulses of different energies in the two undulators. The magnetic chicane delays the electrons with respect to the X-rays, thus introducing a controllable delay between the first and second X-ray pulses.

Figure 5 shows the results of such a double-pulse ESASE experiment at LCLS. Two pulses with an average pulse energy of 6 μJ each and an energy separation of 15 eV were generated (see Fig. 5 b). The timing jitter between the two pulses was not measured but numerical simulations indicate that it is shorter than the individual pulse duration. We note that the energy separation range in our experiment is limited by the tuning range of the LCLS undulator (roughly 3% of the photon energy [59]), but this scheme could be used with variable gap undulators and allow fully independent tuning of the two colors. This will be possible with the upcoming LCLS-II upgrade, enabling continuous tuning between 250 eV and 1200 eV [62]. The temporal separation can be varied from a minimum of 2 fs up to a maximum of roughly 50 fs. Smaller delays could be accessed with a gain-modulation scheme [61]. Improved two-color operation with higher peak power and delay control through overlap could be achieved with a modest upgrade of the XLEAP setup [56].

Using the split-undulator scheme shown in Fig. 5 a, one can also generate two pulses of the same photon energy and with mutual phase stability. Unlike the case of two different colors, where the two pulses are seeded by noise at different frequencies and are uncorrelated, in this case the beam microbunching that generates the first pulse is re-used to generate a second pulse and the two are phase-locked. Figure 5c shows the measured spectra under these conditions. The spectra exhibit stable and repeatable fringes, which implies that the phase between the two pulses is stable to better than the X-ray wavelength. From the variation in the spectral fringes we can infer a phase jitter of 0.77 rad, or 0.5 as between the pulses. In this case the delay can be varied from 0 fs to roughly 5 fs. Beyond this value the delay chicane will destroy the X-ray microbunching and hence the phase stability of the pulses.

SUMMARY AND CONCLUSIONS

We have demonstrated tunable sub-femtosecond X-ray pulses with tens of gigawatts of peak power using a free-electron laser. The pulses were generated by an electron bunch modulated by interaction with a high-power infrared light pulse and compressed in a small magnetic chicane. To diagnose the temporal structure of these pulses we used an attosecond streak camera and measured a median pulse duration of 284 as (476 as) at 905 eV (570 eV). With an eye towards pump/probe experiments, pairs of sub-fs pulses were demonstrated

using a split undulator technique, showing control of the delay and energy separation, but with a reduced peak power compared to the single-pulse case.

These pulses have pulse energies six orders of magnitude higher than what can be achieved with HHG based sources in the same wavelength range. The measured peak power is in the tens to hundreds of gigawatts. Such a marked increase in pulse energy will enable a suite of non-linear X-ray spectroscopy methods such as attosecond-pump/attosecond-probe experiments [63, 64] and four-wave mixing protocols [58] that would be impossible with any other existing attosecond source. Moreover, the achieved photon flux is will enable single-shot X-ray imaging at the attosecond timescale. Finally, the XLEAP setup is based on a passive modulator and it is naturally scalable to the MHz-repetition rate envisioned for the next generation of X-ray free-electron lasers [35, 62].

METHODS

FEL Setup. The x-ray free-electron laser (XFEL) at the Linac Coherent Light Source (LCLS) is composed of a high-brightness linear accelerator (linac) and a magnetic undulator. The XLEAP beamline is composed of a long-period wiggler and a magnetic chicane prior to the undulator section. The accelerator and undulator/wiggler parameters used in this experiment are summarized in Table 1 of the supplemental material. X-rays generated in the undulators are focused with a pair of Kirkpatrick-Baez mirrors to a spot size of approximately ~ 55 μm diameter (FWHM). More information of the FEL parameters is given in the Supplementary Material.

Streaking Laser Setup. The streaking laser pulse is derived from a 120 Hz titanium-doped sapphire laser system synchronized to the accelerator. Ten mJ, 800 nm laser pulses are compressed to ~ 40 fs, and the compressed pulse is used to pump an optical parametric amplifier (TOPAS-HE, Light Conversion) which produces 500 μJ pulses at a wavelength of 1300 nm. The 1300 nm pulse is spectrally filtered to remove any residual pump light or any other colors made by the OPA. A quarter waveplate (Thorlabs AQWP05M-1600) is used to produce circularly polarized laser pulses, which are then focused with a $f = 750$ mm CaF_2 lens. A dichroic mirror (R1300/T400-550) is used to steer the beam into a vacuum chamber. The streaking laser field is combined with the FEL beam using a silver mirror with a 2 mm drilled hole, and both pulses come to a common focus in the interaction region of

a co-axial velocity map imaging (c-VMI) apparatus [49]. The laser is focused to a diameter of $\sim$ 110 μm. More information on the laser configuration along with additional figures showing the experimental geometry are available in the Supplementary Material.

Photoelectron Spectrometer. Our experiment was performed at the Atomic, Molecular, and Optical physics (AMO) beamline of the Linac Coherent Light Source (LCLS). Photoelectrons produced by two-color ionization are collected in our co-axial velocity map imaging (c-VMI) apparatus [49]. Photoelectrons are extracted in the direction opposite to the laser propagation direction, as shown in the supplemental material. Extracted electrons are detected with a microchannel plate detector coupled to a P43 phosphor screen. The phosphor screen is imaged onto a high-speed CCD camera (Opal1k) via the 2 mm holey mirror which couples the streaking laser into the chamber, and through the dichroic mirror. The CCD camera records images of the phosphor screen at the repetition rate of the accelerator, 120 Hz. A target gas is introduced via a molecular beam source, which crosses with the FEL and streaking laser beams in the interaction region. For the two x-ray photon energies considered in the main text, we use neon as the target for 905 eV pulses and CO_2 as the target for 570 eV pulses. More information on the expeimental setup and analysis of the measured photoelectrom momentum distribution is given in the supplemental material.

Data Availability. A subset of the raw data used to produce the figures 2-5 is publicly available at FigShare [link to be added later]. This repository also contains a copy of the analysis script used to invert the photoelectron momentum distributions.

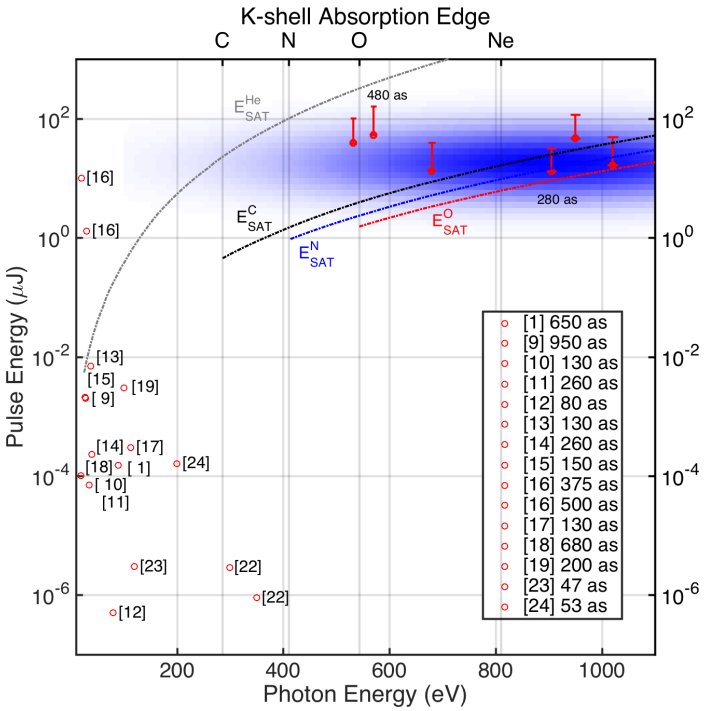

FIG. 4. **Comparison to state of the art attosecond sources.** Survey of published isolated attosecond pulse sources [1, 9–19, 22–24] extending into the soft X-ray domain (red open circles), along with the results demonstrated in this work for a number of different photon energies (red filled circles). The filled circle shows the average pulse energy recorded during the experiment, the error bar extends from the central energy and includes up to 90% of the recorded pulse energies. All previous results were obtained via strong-field driven high harmonic generation with near-infrared and mid-infrared laser fields, while our results are obtained using a free-electron laser (FEL) source. As a first-order estimate of the propensity for nonlinear science (pump/probe spectroscopy, etc.) we show the pulse energy required to saturate $1s$ ionization of carbon (dash-dot, black), nitrogen (dash-dot, blue), oxygen (dash-dot, red), and helium (dash-dot, gray), assuming a 1 μm^2 focal spot size, as a function of X-ray photon energy. Sources within 2 orders of magnitude of the line are likely sources for pump-probe studies. The table in the bottom right corner gives the published pulse duration for the previous measurements. The shaded blue area shows the operational range predicted for LCLS-II.

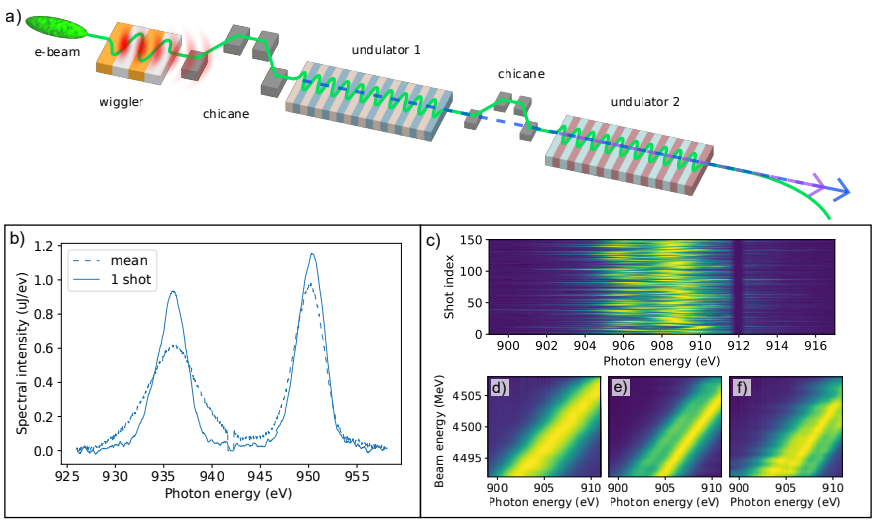

FIG. 5. **Double pulse measurements.**(a): Schematic representation of the double pulse generation experiment. The electron beam is modulated and compressed in the XLEAP beamline and sent to the LCLS undulator. The undulator is divided in two parts separated by a magnetic chicane. Each half of the undulator is used to generate an X-ray pulse with different pulse energies, and the chicane introduces a variable delay between the pulses. (b): Single shot and average two-color spectra measured with a grating spectrometer. (c): Single-shot measurements of the spectrum of the pulse pair with 1 fs delay. The repeatable spectral fringe demonstrate phase stability between the pulses. (d), (e), (f): Averaged phase-stable double shot spectra as a function of photon energy and electron beam energy for a nominal chicane delay of 0 fs (single pulse)(d), 0.5 fs (e) and 3 fs (f).

SUPPLEMENTARY MATERIALS

Materials and Methods

Supplementary Text

Figs. S1 to S12

References *(65-78)*

---

[1] M. Hentschel, *et al.*, *Nature* **414**, 509 (2001).

[2] X. F. Li, A. LHuillier, M. Ferray, L. A. Lompr, G. Mainfray, *Physical Review A* **39**, 5751 (1989).

[3] J. L. Krause, K. J. Schafer, K. C. Kulander, *Physical Review Letters* **68**, 3535 (1992).

[4] P. B. Corkum, *Physical Review Letters* **71**, 1994 (1993).

[5] M. Chini, K. Zhao, Z. Chang, *Nature Photonics* **8**, 178 (2014).

[6] P. B. Corkum, F. Krausz, *Nature Physics* **3**, 381 (2007).

[7] Z. Chang, P. Corkum, *JOSA B* **27**, B9 (2010).

[8] M. F. Ciappina, *et al.*, *Reports on Progress in Physics* **80**, 054401 (2017).

[9] T. Sekikawa, A. Kosuge, T. Kanai, S. Watanabe, *Nature* **432**, 605 (2004).

[10] G. Sansone, *et al.*, *Science* **314**, 443 (2006).

[11] I. J. Sola, *et al.*, *Nature Physics* **2**, 319 (2006).

[12] E. Goulielmakis, *et al.*, *Science* **320**, 1614 (2008).

[13] H. Mashiko, *et al.*, *Physical Review Letters* **100**, 103906 (2008).

[14] X. Feng, *et al.*, *Physical Review Letters* **103**, 183901 (2009).

[15] F. Ferrari, *et al.*, *Nature Photonics* **4**, 875 (2010).

[16] E. J. Takahashi, P. Lan, O. D. Mcke, Y. Nabekawa, K. Midorikawa, *Nature Communications* **4**, 2691 (2013).

[17] M. Ossiander, *et al.*, *Nature Physics* **13**, 280 (2017).

[18] T. R. Barillot, *et al.*, *Chemical Physics Letters* **683**, 38 (2017).

[19] B. Bergues, *et al.*, *Optica* **5**, 237 (2018).

[20] O. Jahn, *et al.*, *Optica* **6**, 280 (2019).

[21] D. Attwood, A. Sakdinawat, *X-rays and extreme ultraviolet radiation: principles and applications* (Cambridge university press, 2017).

[22] S. M. Teichmann, F. Silva, S. L. Cousin, M. Hemmer, J. Biegert, *Nature Communications* **7**, 11493 (2016).

[23] T. Gaumnitz, *et al.*, *Optics Express* **25**, 27506 (2017).

[24] J. Li, *et al.*, *Nature Communications* **8**, 186 (2017).

[25] A. S. Johnson, *et al.*, *Science Advances* **4**, eaar3761 (2018).

[26] T. J. A. Wolf, *et al.*, *Nature Communications* **8**, 29 (2017).

[27] S. P. Neville, M. Chergui, A. Stolow, M. S. Schuurman, *Physical Review Letters* **120**, 243001 (2018).

[28] A. R. Attar, *et al.*, *Science* **356**, 54 (2017).

[29] W. Ackermann, *et al.*, *Nature photonics* **1**, 336 (2007).

[30] P. Emma, *et al.*, *Nat Photon* **4**, 641 (2010).

[31] E. Allaria, *et al.*, *Nat Photon* **6**, 699 (2012).

[32] E. Allaria, *et al.*, *Nat Photon* **7**, 913 (2013).

[33] T. Ishikawa, H. Aoyagi, T. Asaka, al., *Nat Photon* **6**, 540 (2012).

[34] H.-S. Kang, *et al.*, *Nature Photonics* **11**, 708 (2017).

[35] M. Altarelli, *Nuclear Instruments and Methods in Physics Research Section B: Beam Interactions with Materials and Atoms* **269**, 2845 (2011).

[36] R. Bonifacio, C. Pellegrini, L. Narducci, *Optics Communications* **50**, 373 (1984).

[37] C. Pellegrini, A. Marinelli, S. Reiche, *Rev. Mod. Phys.* **88**, 015006 (2016).

[38] Z. Huang, K.-J. Kim, *Phys. Rev. ST Accel. Beams* **10**, 034801 (2007).

[39] R. Bonifacio, L. De Salvo, P. Pierini, N. Piovella, C. Pellegrini, *Phys. Rev. Lett.* **73**, 70 (1994).

[40] S. Huang, *et al.*, *Physical review letters* **119**, 154801 (2017).

[41] A. Marinelli, *et al.*, *Applied Physics Letters* **111**, 151101 (2017).

[42] C. Behrens, *et al.*, *Nature Communications* **5**, 3762 (2014).

[43] N. Hartmann, *et al.*, *Nature Photonics* **12**, 215 (2018).

[44] A. A. Zholents, *Physical Review Special Topics - Accelerators and Beams* **8**, 040701 (2005).

[45] A. A. Zholents, W. M. Fawley, *Phys. Rev. Lett.* **92**, 224801 (2004).

[46] E. Hemsing, G. Stupakov, D. Xiang, A. Zholents, *Reviews of Modern Physics* **86**, 897 (2014).

[47] J. MacArthur, *et al.*, *Submitted to Phys. Rev. Lett.* (2019).

[48] J. MacArthur, J. Duris, Z. Huang, A. Marinelli, Z. Zhang, *Proc. 9th International Particle Accelerator Conference (IPAC'18), Vancouver, BC, Canada, April 29-May 4, 2018*, no. 9 in International Particle Accelerator Conference (JACoW Publishing, Geneva, Switzerland, 2018), pp. 4492–4495. Https://doi.org/10.18429/JACoW-IPAC2018-THPMK083.

[49] S. Li, *et al.*, *AIP Advances* **8**, 115308 (2018).

[50] R. Kienberger, *et al.*, *Nature* **427**, 817 (2004).

[51] A. K. Kazansky, A. V. Bozhevolnov, I. P. Sazhina, N. M. Kabachnik, *Physical Review A* **93**, 013407 (2016).

[52] A. K. Kazansky, I. P. Sazhina, V. L. Nosik, N. M. Kabachnik, *Journal of Physics B: Atomic, Molecular and Optical Physics* **50**, 105601 (2017).

[53] S. Li, *et al.*, *Optics Express* **26**, 4531 (2018).

[54] J. Itatani, *et al.*, *Physical Review Letters* **88**, 173903 (2002).

[55] J. M. Glownia, *et al.*, *Optics Express* **18**, 17620 (2010).

[56] Z. Zhang, J. Duris, J. P. MacArthur, Z. Huang, A. Marinelli, *Phys. Rev. Accel. Beams* **22**, 050701 (2019).

[57] Y. Ding, Z. Huang, D. Ratner, P. Bucksbaum, H. Merdji, *Phys. Rev. ST Accel. Beams* **12**, 060703 (2009).

[58] S. Mukamel, D. Healion, Y. Zhang, J. D. Biggs, *Annual Review of Physical Chemistry* **64**, 101 (2013).

[59] A. A. Lutman, *et al.*, *Phys. Rev. Lett.* **110**, 134801 (2013).

[60] T. Hara, *et al.*, *Nat Commun* **4** (2013).

[61] A. Marinelli, *et al.*, *Physical Review Letters* **111**, 134801 (2013).

[62] R. Schoenlein, New Science Opportunities Enabled by LCLS-II X-ray Lasers (2015).

[63] S. R. Leone, *et al.*, *Nature Photonics* **8**, 162 (2014).

[64] I. V. Schweigert, S. Mukamel, *Physical Review A* **76**, 012504 (2007).

ACKNOWLEDGEMENTS

The authors would like to acknowledge Tais Gorkhover, Christoph Bostedt, Jon Marangos, Claudio Pellegrini, Adrian Cavalieri, Nora Berrah, Linda Young, Lou DiMauro, Heinz-Dieter Nuhn, Gabriel Marcus, and Tim Maxwell for useful discussions and suggestions. We

would also like to acknowledge Michael Merritt, Oliver Schmidt, Nikita Strelnikov, Isaac Vasserman for their assistance in designing, constructing and installing the XLEAP wiggler. We also acknowledge the SLAC Accelerator Operations group, and the Mechanical and Electrical engineering divisions of the SLAC Accelerator Directorate, especially Gene Kraft, Manny Carrasco, Antonio Cedillos, Kristi Luchini and Jeremy Mock for their invaluable support.

This work was supported by U.S. Department of Energy Contracts No. DE-AC02-76SF00515, DOE-BES Accelerator and detector research program Field Work Proposal 100317, DOE-BES, Chemical Sciences, Geosciences, and Biosciences Division, and Department of Energy, Laboratory Directed Research and Development program at SLAC National Accelerator Laboratory, under contract DE-AC02-76SF00515. WH acknowledges financial support by the BACATEC programme. P.R. and M.F.K. acknowledge additional support by the DFG via KL-1439/10, and the Max Planck Society. G. H. acknowledges the Deutsche Forschungsgemeinschaft (DFG, German Research Foundation) Projektnummer 328961117 SFB 1319 ELCH.